Geophys. J. R. astr. Soc. (1982) **69**, 383–404

Upper mantle anisotropy: evidence from free oscillations

Don L. Anderson *Seismological Laboratory, California Institute of Technology, Pasadena, California 91125, USA*

Adam M. Dziewonski *Department of Geological Sciences, Harvard University, Cambridge, Massachusetts 02138, USA*

Received 1981 September 21; in original form 1981 May 22

Summary. Isotropic earth models are unable to provide uniform fits to the gross Earth normal mode data set or, in many cases, to regional Love- and Rayleigh-wave data. Anisotropic inversion provides a good fit to the data and indicates that the upper 200 km of the mantle is anisotropic. The nature and magnitude of the required anisotropy, moreover, is similar to that found in body wave studies and in studies of ultramafic samples from the upper mantle. Pronounced upper mantle low-velocity zones are characteristic of models resulting from isotropic inversion of global or regional data sets. Anisotropic models have more nearly constant velocities in the upper mantle.

Normal mode partial (Frechét) derivatives are calculated for a transversely isotropic earth model with a radial axis of symmetry. For this type of anisotropy there are five elastic constant. The two shear-type moduli can be determined from the toroidal modes. Spheroidal and Rayleigh modes are sensitive to all five elastic constants but are mainly controlled by the two compressional-type moduli, one of the shear-type moduli and the remaining, mixed-mode, modulus. The lack of sensitivity of Rayleigh waves to compressional wave velocities is a characteristic only of the isotropic case. The partial derivatives of the horizontal and vertical components of the compressional velocity are nearly equal and opposite in the region of the mantle where the shear velocity sensitivity is the greatest. The net compressional wave partial derivative, at depth, is therefore very small for isotropic perturbations. Compressional wave anisotropy, however, has a significant effect on Rayleigh-wave dispersion. Once it has been established that transverse anisotropy is important it is necessary to invert for all five elastic constants. If the azimuthal effect has not been averaged out a more general anisotropy may have to be allowed for.

Introduction

There is a growing body of evidence that much of the upper mantle may be anisotropic to the propagation of seismic waves. The early evidence was the discrepancy between Rayleigh-

and Love-wave dispersion (Anderson 1961, 1966; Anderson & Harkrider 1962) and the azimuthal dependence of oceanic P_n velocities (Raitt, Shor & Morris 1971; Hess 1964). Azimuthal variations have now been documented for many areas of the world (Bibee & Shor 1976; Bamford 1977) and the Rayleigh–Love discrepancy is also widespread (McEvilly 1964; Aki 1968; Forsyth 1975; Yu & Mitchell 1979; Schlue & Knopoff 1977). Shear-wave birefringence, a manifestation of anisotropy, has also been reported (Anderson 1966; Hirn 1977; Ando, Ishikawa & Wada 1980). The degree of anisotropy varies but is typically about 5 per cent. It is not known to what depth the anisotropy extends but some of the data (e.g. Ando *et al.* 1980; Hirn 1977) requires it at depths as great as 200 km.

Anderson (1966) proposed that the 'discrepancy' between mantle Rayleigh and Love waves could be explained if the vertical P and S velocities in the upper mantle were 7–8 per cent less than the horizontal velocities. He also showed that models without an upper mantle low-velocity zone, such as the Jeffreys model, could satisfy the dispersion data if the upper mantle was anisotropic. The Love–Rayleigh discrepancy has survived to the present and models have been proposed which have SV in the upper mantle less than SH by about 4 per cent. These more recent models, however, are based on separate isotropic inversions of Love and Rayleigh waves and therefore do not indicate the true anisotropy. We will show that there is a trade-off between anisotropy and structure. In particular the very low shear velocities, 4.0–4.2 km s^{-1}, found by most isotropic and pseudo-isotropic inversions, are not a characteristic of models resulting from full anisotropic inversion of the same data. The P-wave anisotropy also makes a significant contribution to Rayleigh-wave dispersion. This has been ignored in recent inversion attempts. Finally, sphericity needs to be taken into account.

Since intrinsic anisotropy requires both anisotropic crystals and preferred orientation, the anisotropy of the mantle contains information about the mineralogy and the flow. For example, olivine, the most abundant upper mantle mineral, is extremely anisotropic for both P- and S-wave propagation. Apparently it is easily oriented by the ambient stress or flow field. Olivine-rich outcrops show a consistent preferred orientation over large areas. In general, the seismically fast axes are in the plane of the flow with the a-axis, the fastest direction, pointing in the direction of flow. The b-axis, the minimum velocity direction, is generally normal to the flow plane. The petrological data are summarized in Peselnick & Nicolas (1978) and Christensen & Salisbury (1979).

The magnitude of the anisotropy in the mantle is comparable to that found in ultramafic rocks. Soft layers or oriented fluid-filled cracks also give an apparent anisotropy but these need to be involved only for very low velocities. Much seismic data that are used in upper mantle modelling are averages over several tectonic provinces or averages over many azimuths. Azimuthal anisotropy may therefore be averaged out but differences between vertical and horizontal velocities are not.

The presence of anisotropy is not only of theoretical interest as a second-order effect. If the upper mantle is, in fact, anisotropic then isotropic inversion of seismic data will result in erroneous structures because of improper parameterization. Such important seismological problems as the presence and nature of a low-velocity zone and the depth extent of differences between oceans and continents depend critically on the validity of the assumption of isotropy (Anderson 1966, 1979). It is the purpose of this paper to demonstrate the effect of anisotropy on surface waves and free oscillations and the trade-offs between structure and anisotropy. This is conveniently accomplished by the use of partial or Frechét derivatives (e.g. Jeffreys 1961; Anderson 1964, 1967) which have played an important role in earth structure modelling and inversion of seismic data. Partial derivative diagrams succinctly summarize the effect of the various parameters on normal mode periods or surface wave dispersion.

Transverse isotropy

A solid characterized by an axis of symmetry is termed transversely isotropic and exhibits the same symmetry as a hexagonal crystal. It is described by five elastic constants. Pure longitudinal and shear waves propagate in the symmetry plane and along the symmetry axis and measurements of velocities in these two orthogonal directions determine four of the five elastic constants. At intermediate directions there are three coupled elastic wave modes and the velocities of these involve the fifth constant.

The five elastic constants can also be determined by measuring the toroidal and spheroidal normal mode spectra. Toroidal modes are sensitive to the two shear-type moduli and spheroidal modes are sensitive primarily to four of the five moduli.

Transverse isotropy, although a special case of anisotropy, has quite general applicability in geophysical problems. This kind of anisotropy is exhibited by laminated or finely layered solids (Postma 1955; Anderson 1961, 1962, 1966; Backus 1962), solids containing oriented cracks or melt zones (Anderson, Minster & Cole 1974), peridotite massifs, harzburgite bodies (Christensen & Salisbury 1979), the oceanic upper mantle (Christensen & Crosson 1968), and floating ice sheets (Anderson 1961). A mantle containing small-scale layering, sills or randomly oriented dykes will also appear to be macroscopically transversely isotropic. If flow in the upper mantle is mainly horizontal then the evidence from fabrics of peridotite nodules and massifs suggest that the average vertical velocity will be less than the average horizontal velocity and horizontally propagating *SH*-waves will travel faster than *SV*-waves. In regions of upwelling and subduction the slow direction may not be vertical but if these regions are randomly oriented the average earth will still display the spherical equivalent of transverse isotropy. Since the upper mantle is composed primarily of the very anisotropic crystals, olivine and pyroxene, and since these crystals tend to align themselves in response to flow and non-hydrostatic stresses, it is likely that the upper mantle is anisotropic to the propagation of elastic waves. Although the preferred orientation in the horizontal plane can be averaged out by determining the velocity in many directions, or over many plates with different motion vectors, the vertical still remains a unique direction.

If anisotropy persists to moderate depth then it must be allowed for in gross earth and regional inversions as well as in more local studies. The large-scale mantle motions responsible for plate tectonics, combined with the ease of dislocation creep at the high temperatures in the upper mantle, can be expected to orient the crystals in the mantle. In a crystalline solid the crystals must be oriented at random in order to be isotropic. There is no particular reason for believing that this is true in the mantle. Since isotropy is a degenerate case it cannot be assumed that models resulting from isotropic inversion are even approximately correct.

The inconsistency between Love- and Rayleigh-wave data, first noted for global data, has now been found in regional data sets. The possibility of Love-wave higher mode interference (Anderson & Toksöz 1963; Thatcher & Brune 1969) complicates the interpretation but can be ruled out in some cases. It appears that lateral heterogeneity is not responsible for the Love–Rayleigh-wave discrepancy and that anisotropy is an intrinsic and widespread property of the uppermost mantle. The crust and exposed sections of the upper mantle exhibit layering on scales ranging from metres to kilometres. Such layering in the mantle would be beyond the resolution of seismic waves and would show up as an apparent anisotropy. This, plus the preponderance of aligned olivine in mantle samples, means that at least five elastic constants are required to properly describe the elastic response of the upper mantle. It is clear that inversion of *P*-wave data, for example, or even of *P* and *SV* data cannot provide all of these constants. Even more serious, inversion of a limited data set, with the assumption of isotropy, does not necessarily yield the proper structure. The variation of

velocities with angle of incidence, or ray parameter, will be interpreted as a variation of velocity with depth. In principle, simultaneous inversion of Love- and Rayleigh-wave data can help resolve the ambiguity.

The theory of surface wave propagation in a layered transversely isotropic solid was developed by Anderson (1961, 1962, 1966) and Harkrider & Anderson (1962). The effect of sphericity was treated by Takeuchi & Saito (1972). Propagation in the axial directions of a medium displaying orthorhombic symmetry was treated by Anderson (1966) and Toksöz & Anderson (1963). For Love waves isotropic theory can be generalized easily to the anisotropic case. The shear moduli determined from isotropic inversion of Love waves is a simple function of the two anisotropic shear moduli. An equivalent isotropic model can therefore always be found that will satisfy Love wave and toroidal mode data. No such simple transfomation is possible for Rayleigh waves. Models found from isotropic inversion of Rayleigh-wave data are not necessarily even approximately similar to the real anisotropic Earth. If four or five elastic constants plus density are necessary to describe the Earth at a given depth and only two or three parameters are allowed to vary, it is obvious that the problem is underparameterized. An isotropic inversion scheme will result in perturbations of the available parameters and may result in a model exhibiting oscillatory or rough structure that is not a characteristic of the real Earth. If accurate spheroidal and toroidal data are available, systematic deviations from predicted periods for the best fitting isotropic model may be symptomatic of anisotropy. Other symptoms may be unreasonable P_n and S_n velocities or velocity and density reversals. Some or all of the above are characteristics of all gross earth inversion attempts to date. In some areas, e.g. Canadian Shield, there is little or no discrepancy between Love and Rayleigh waves (Brune & Dorman 1963).

Inversion results

We will refer to normal modes, teleseismic travel times and great circle surface wave dispersion data as the gross earth data set. By combining data from many earthquakes and stations it is hoped that lateral variations and azimuthal effects can be averaged out. Such problems as regional variations and their depth extent can then be discussed in terms of variations from the average earth. It has been surprisingly difficult to find a spherically symmetric earth model that satisfies the entire gross earth data set. The normal mode models did not satisfy body wave data until it was recognized that absorption made the 'elastic' constants frequency-dependent (Akopyan, Zharkov & Lyubimova 1975; Randall 1976; Liu, Anderson & Kanamori 1976; Kanamori & Anderson 1977) as originally proposed by Jeffreys (1965). Even when absorption was allowed for, gross earth models did not satisfy the complete data set. The most obvious problem is the well-known Rayleigh wave–Love wave discrepancy (Anderson 1966). The earth models B1, 1066 and C2 (Jordan & Anderson 1974; Gilbert & Dziewonski 1975; Anderson & Hart 1976a) were the result of isotropic inversion of large normal mode data sets. These models did not satisfy shear wave travel-time data or short-period, < 200 s, Love- and Rayleigh-wave data. The inclusion of attenuation made it possible to reconcile the free oscillation and body wave data (Anderson *et al.* 1976; Anderson & Hart 1976b; Hart, Anderson & Kanamori 1977; Dziewonski, Hales & Lapwood 1975). The earth models QM1, QM2 and PEM, derived by these authors, satisfied a large variety of data but they still disagreed with the mantle Love- and Rayleigh-wave observations. This suggests that the assumption of isotropy in the upper mantle may be in error.

Dziewonski & Anderson (1981) inverted a large data set consisting of about 1000 normal mode periods, 500 summary travel-time observations, 100 normal mode Q values, mass and moment of inertia to obtain the radial distribution of elastic properties, Q values and density

in the Earth's interior. By allowing for transverse isotropy in the upper 200 km of the mantle they were able to satisfy, to high precision, teleseismic travel times and normal mode periods and, at the same time, Love- and Rayleigh-wave dispersion to periods as short as 70 s. The model is isotropic below a depth of 220 km. There was no need to extend the anisotropy deeper. The upper mantle is characterized by a 2–4 per cent anisotropy in velocity and a slight variation of the five elastic constants with depth. A similar structure satisfies dispersion data for Pacific ocean paths. Although a high-velocity LID, $V_S > 4.6\,\mathrm{km\,s^{-1}}$, is not required to satisfy the mantle surface wave data such a LID with thickness ~ 20–40 km is needed to satisfy the shorter period, $T < 70$ s, Rayleigh-wave data and S_n data. This is much thinner than the LID thickness in isotropic models.

In the PREM inversion a satisfactory fit to the gross earth data set, including mantle Love and Rayleigh waves, was achieved with a linear gradient in all five elastic constants between Moho and 220 km. *PH*, *PV* and *SH* decrease slightly and *SV* increases slightly with depth. Different pressure and temperature derivatives or a change of crystal orientation with depth are required if these differences in slope are real. The overall anisotropy decreases with depth. This is in marked contrast to the results of isotropic inversion which invariably give a pronounced shear wave low-velocity zone with $V_S = 4.0$–$4.2\,\mathrm{km\,s^{-1}}$. The anisotropic models have average anisotropies in the upper 200 km of the mantle of about 3 per cent.

The introduction of anisotropy into the upper mantle introduces more degrees of freedom into the inversion problem. Dziewonski & Anderson (1981) were able to fit the gross earth data set with an earth model that had 13 radial subdivisions. The density and elastic wave velocities in each region were described by low-order polynomials. A total of 92 parameters were sufficient to satisfy the data. The locations of the boundaries are additional parameters making a total of 105 parameters. Some of the parameters such as radius of the Earth, radius of the inner core, average depth to Moho, mass of the Earth, etc. were determined from other data. Dziewonski & Anderson (1981) also attempted to fit the same data set with isotropic inversion but were unsuccessful.

In the anisotropic modelling, the upper mantle, to a depth of 220 km, required 12 parameters for its description. These are the density, the five elastic constants and a linear gradient of each. In the isotropic modelling this region had to be split into two, also giving 12 parameters, which involves a two-parameter description of density and the two elastic constants in each region. Even the best fitting isotropic models, however, were unable to fit the short period (< 200 s) Love- and Rayleigh-wave data. The isotropic inversion also resulted in a large and unreasonable mean crustal thickness. The overall fit to the normal mode data set is also inferior for the isotropic model. The superior fit achieved by anisotropic modelling is not due to an increase in the number of parameters. The anisotropic parameters are only a small fraction of the total number of parameters in the model and the same number of parameters are used for both the isotropic and anisotropic inversions.

Partial derivatives

The parameter variation equations for transversely isotropic media are given in Takeuchi & Saito (1972) and Dziewonski & Anderson (1981). In Figs 1–16 we give the relative change in a normal mode period due to a change in parameters, plotted as a function of depth.

We shall compare, for a number of modes, partial derivatives for a transversely isotropic structure with those for an isotropic earth. The most striking differences between these two sets of partials are: (1) substantial sensitivity of spherical modes to perturbations in *VPV* and *VPH* at depths for which the partial for the isotropic velocity *VP* is practically zero; and (2) different sensitivity of spherical and toroidal overtones to perturbations in *VSV* and *VSH*.

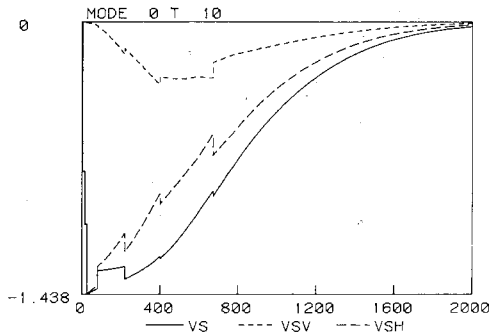

Figure 1. Partial derivatives showing relative change in normal mode period due to a change in shear velocity in a 1 km thick shell as a function of depth. Vertical scale is RdT/TdV; horizontal scale gives depth in km. The solid line gives the isotropic partial derivative. The dashed lines give the effect of perturbations in two components of the velocity. In the case of shear waves the horizontal shear velocities are *VSV* and *VSH*; the vertical shear velocity is *VSV*. Period of ${}_0T_{10}$ is about 620 s. R is 6371 km.

Both of these effects can be examined by consideration of the expressions associated with the appropriate kernels and their asymptotic properties (see Appendix).

Four of the five elastic constants can be expressed in terms of the velocities in the symmetry plane and along the symmetry axis, taken as vertical. The symmetry plane is actually a spherical surface and 'vertical' is the radial direction.

We have calculated partial derivitives for the following parameters:

$$VPH = (A/\rho)^{1/2},$$

$$VPV = (C/\rho)^{1/2},$$

$$VSH = (N/\rho)^{1/2},$$

$$VSV = (L/\rho)^{1/2},$$

$$\eta = F/(A - 2L).$$

A transversely isotropic solid has the symmetry of a hexagonal crystal with the c-axis being the symmetry direction. In compact tensor notation $A = C_{11}$, $C = C_{33}$, $L = C_{44}$, $F = C_{13}$ and $N = (C_{11}\text{-}C_{12})/2$. The velocities of the elastic waves depend on direction relative to the symmetry axis, taken as the radial direction. *VSV* corresponds to the velocity of the vertically travelling shear wave and horizontally propagating shear waves with vertical polarization. *VSH* is the velocity of horizontally propagating *SH*-waves. *VPV* and *VPH* are,

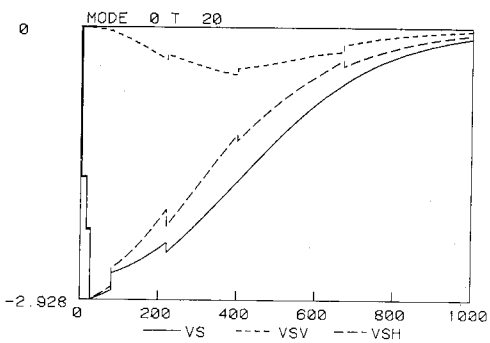

Figure 2. Same as Fig. 1 for mode ${}_0T_{20}$, period about 360 s.

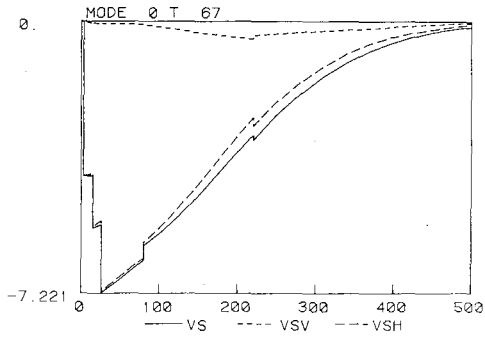

Figure 3. Same as Fig. 1 for mode ${}_0T_{67}$, period about 127 s.

respectively, the vertical and horizontal compressional velocities. F is a modulus that is a function of the velocities at intermediate directions.

The partial derivatives for the fundamental toroidal modes are similar to those for isotropic earth models; see for example tabulations and figures in Anderson (1964, 1967). In fact, the theory developed for isotropic layers can be used for anisotropic layers by a simple transformation (Anderson 1962). Representative shear velocity partial derivatives are given in Figs 1–3. These cover the period range from 620 to 126 s. The main novelty introduced by anisotropy is the slight sensitivity of the low-order modes to *VSV* in the upper mantle. The fundamental toroidal modes are most sensitive to *VSH*. The magnitude of the *SH* partials decreases rapidly with depth. As a rough rule-of-thumb, fundamental mode Love-waves sample to about one-third of a wavelength; this is the half-amplitude point for the *VSH* partial derivatives.

The toroidal overtones, Figs 4–8, illustrate an interesting phenomena. The *SV* and *SH* partials are oscillatory and out of phase. The magnitudes of the two partials are comparable. Toroidal overtones therefore provide information about the angular dependence of the shear velocity. Although toroidal oscillations involve tangential, or *SH* motion, the overtones can be viewed as a superposition of upward and downward travelling waves and therefore are sensitive to the directional dependence of the shear velocity (Anderson 1962). The shear wave partials are oscillatory with depth and become very small below a depth of about $(l+1)/3$ times the wavelength (λ) where l is the azimuthal order number. The spheroidal modes, discussed next, are primarily sensitive to *VSV*, *VPV*, *VPH*, and η and are virtually decoupled from the shear parameter N, which controls the horizontal *SH* velocity and fundamental Love-wave dispersion.

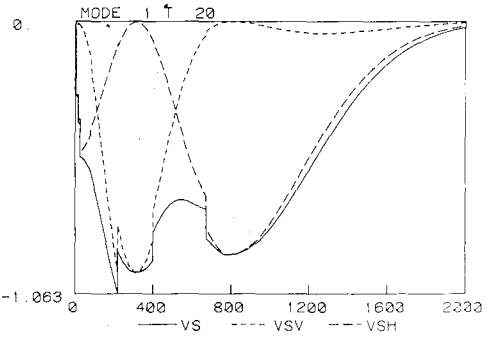

Figure 4. Same as Fig. 1 for mode ${}_1T_{20}$, period about 241 s.

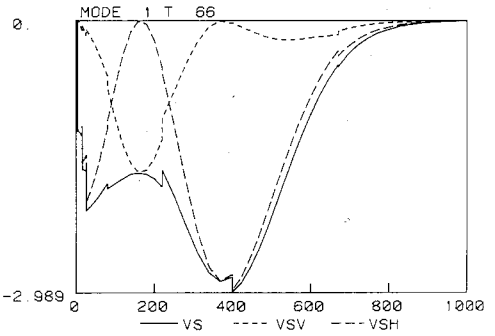

Figure 5. Same as Fig. 1 for mode ${}_1T_{66}$, period about 103 s.

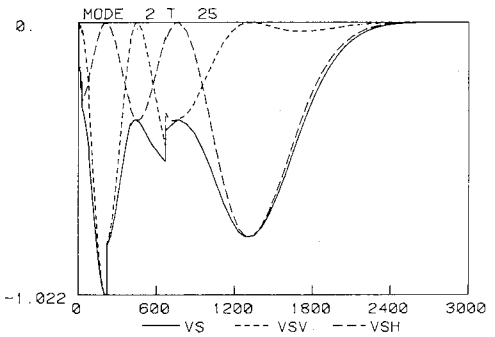

Figure 6. Same as Fig. 1 for mode ${}_2T_{25}$, period about 171 s.

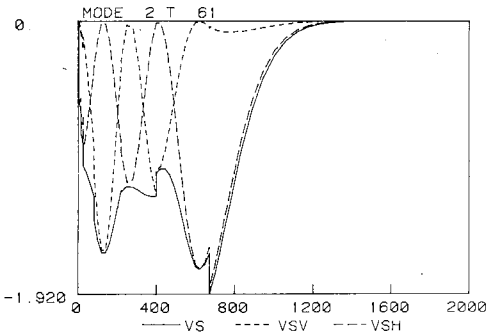

Figure 7. Same as Fig. 1 for mode ${}_2T_{61}$, period about 92 s.

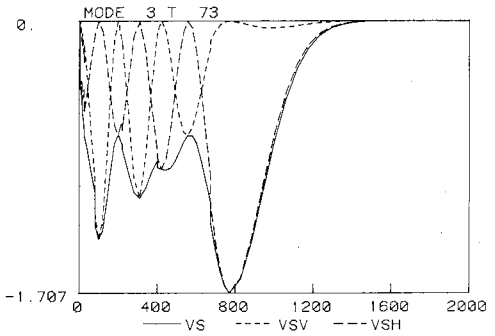

Figure 8. Same as Fig. 1 for mode ${}_3T_{73}$, period about 72 s.

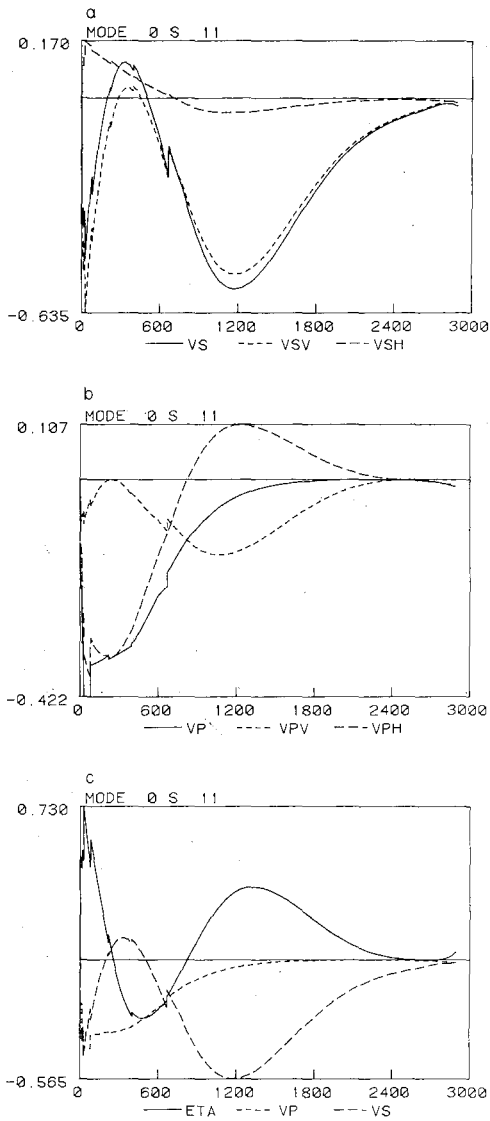

Figure 9. Same as Fig. 1 for mode ${}_0S_{11}$, period about 537 s. (a) The shear wave partial derivatives. (b) The compressional wave partial derivatives. Solid lines in (a) and (b) are for isotropic perturbations. (c) The isotropic compressional wave and shear wave partials (dashed lines) and the η partial (solid line). Note that Rayleigh waves are sensitive to *VSV*, *VPV*, *VPH* and η.

The fundamental mode Rayleigh-wave partial derivatives are very similar in shape and only a few representative examples will be shown. Three figures are shown for each mode. The first figure in each set gives the *VSV*, *VSH* and total (isotropic) shear velocity partial derivatives. *SV* is always more important than *SH* and shows a broad maximum at a depth of about $\lambda/3$. The peak is also about $\lambda/3$ broad so the region of the mantle being sampled extends from about $\lambda/6$ to $\lambda/2$. These modes are also sensitive to *VSV* in the crust and uppermost mantle. The second figure in each set gives the total (isotropic) *VP* partial derivative and the individual components, *VPV* and *VPH*. As is well known, Rayleigh waves are less sensitive to *P*-velocity than to *S*-velocity, except in the uppermost mantle, and the *P*-wave

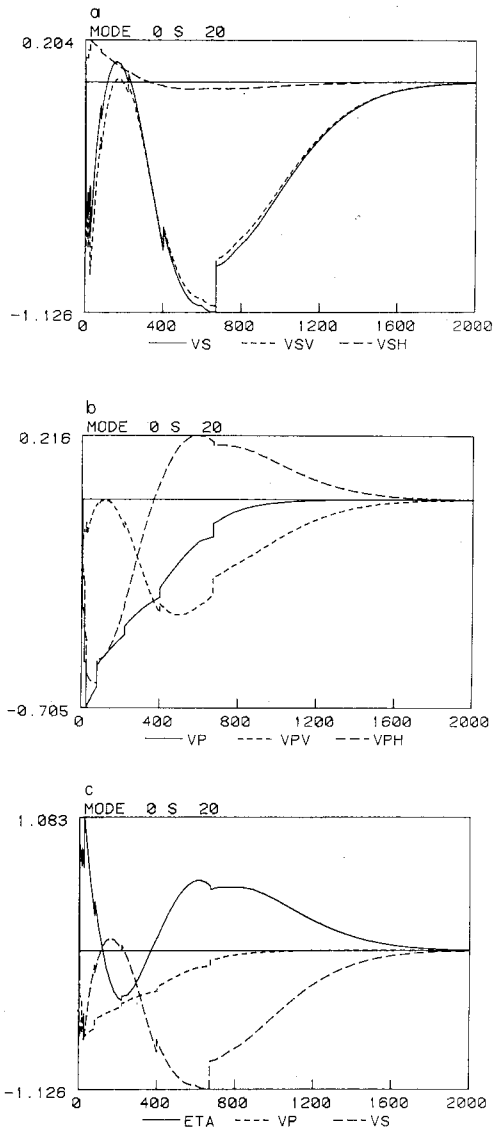

Figure 10. Same as Fig. 9 for mode ${}_0S_{20}$, period about 347 s.

partials decrease rapidly with depth. In isotropic structures the *VP* partials are small below about $\lambda/3$. However, the upper mantle *P*-velocity should be well determined from a large, accurate normal mode data set. Even in isotropic inversion the compressional velocity in the upper mantle should be a free parameter since its effect is not negligible.

Below a depth of about $\lambda/3$ the *VPV* and *VPH* partials are nearly equal and opposite, yielding a very small net effect for isotropic perturbations. The individual partials are large at a depth of about $\lambda/3$. A given fractional *P*-wave anisotropy has about the same effect as a similar relative change in shear velocity. If only fundamental mode Rayleigh-wave data are available there will be a trade-off between upper mantle shear wave velocity and upper mantle compressional wave anisotropy. This can only be resolved with other data, such as toroidal modes, overtones or body waves.

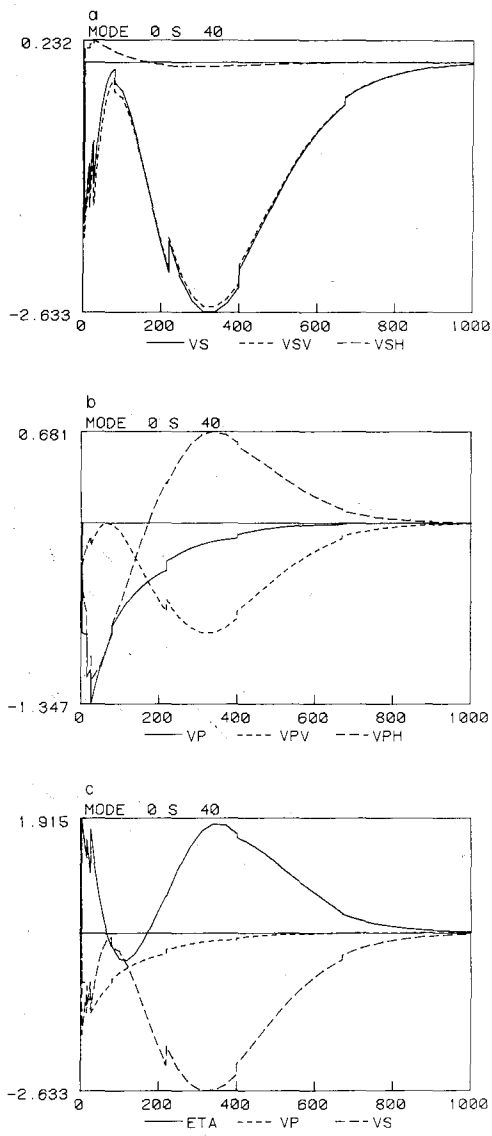

Figure 11. Same as Fig. 9 for mode ${}_0S_{40}$, period about 212 s.

It is clear from these figures that, in an anisotropic earth, Rayleigh waves cannot be assumed to be independent of the compressional velocity. Relative to an isotropic starting model an increase of *VPH* and a decrease of *VPV* have the same effect as a decrease in *VSV*.

In olivine and olivine-rich aggregates the direction of the *b*-axis has relatively slow velocities for both *P*- and *S*-waves. The *a*-axis is a fast direction for both. It cannot be assumed that compressional wave anistropy can be ignored. If only shear velocities are allowed to vary in an inversion scheme, or if the *P*-wave anisotropy is not allowed for, the necessary perturbations in the structure will be larger than if both *P*- and *S*-waves are allowed to contribute in the inversion.

Fig. 9(c) shows the isotropic *VP* and *VS* partial derivatives for mode ${}_0S_{11}$. The effect of the parameter η is also shown. For an isotropic solid η is unity. It is difficult to estimate this

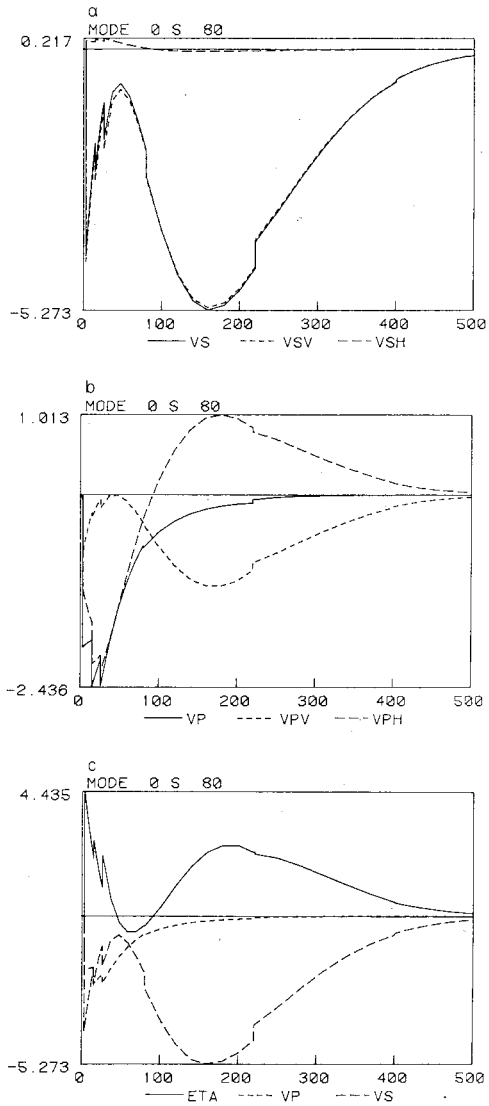

Figure 12. Same as Fig. 9 for mode ${}_0S_{80}$, period about 119 s.

parameter for the mantle, especially from body waves, but it appears to deviate from unity by 10–20 per cent (Anderson 1966; Dziewonski & Anderson 1981). From these results it is clear that mode ${}_0S_{11}$ is primarily sensitive to *VSV*, *VPV*, *VPH* and η. This is generally true for all the spheroidal modes. The longer period modes are slightly sensitive to *VSH* in the upper mantle. Note that for the short-period spheroidal modes, ${}_0S_{80}$ for example, the total shear wave partials are almost entirely due to the *SV* contribution. The individual *VPV* and *VPH* partials, however, continue to be important.

The compressional wave partial derivatives for the first spheroidal overtone, Fig. 13, illustrate the cancellation that occurs for the isotropic case. *VPH* and *VPV* have nearly equal and opposite effects, giving a very small isotropic contribution. In the anisotropic case these modes, however, give good control on the upper mantle compressional velocities. The η partials are similar in shape to the individual shear and compressional wave partials. This

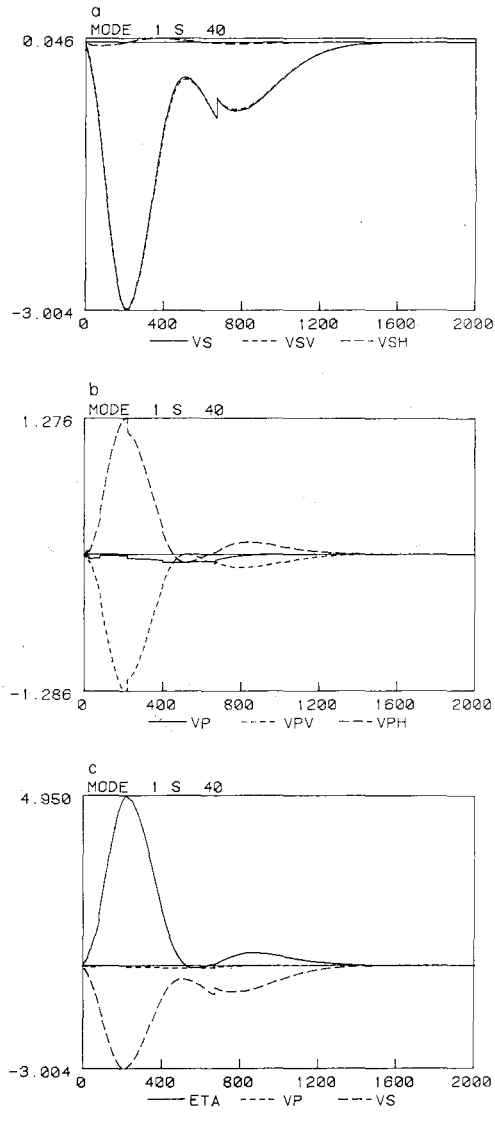

Figure 13. Same as Fig. 9 for mode ${}_1S_{40}$, period about 149 s.

means that a large accurate data set, covering a large frequency band and including many higher modes, is required in order to determine the full set of elastic constants.

The trade-offs between parameters are evident from these plots. For example, a decrease in *VPH*, an increase in *VPV* and an increase in shear velocity in the upper mantle at depths of the order of 1/4 to 1/2 a wavelength, all have similar effects on the fundamental Rayleigh mode. Thus, *P*-wave anisotropy, with $PH > PV$ has an effect similar to an upper mantle shear wave low-velocity zone. Love- and Rayleigh-wave velocities imply that $SH > SV$ in the upper mantle. This is consistent with the *P*-wave anisotropy, i.e. PREM.

Further numerical experiments

The earth model PREM is based on a large data set and should represent a good spherically

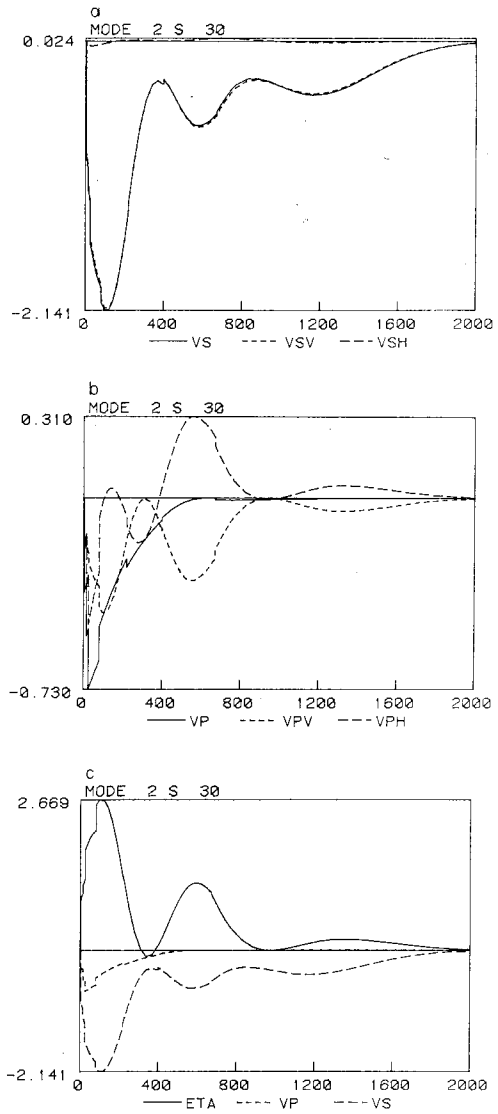

Figure 14. Same as Fig. 9 for mode ${}_2S_{30}$, period about 161 s.

averaged model. In order to investigate the effect of anisotropy over a more homogeneous path we have compiled oceanic dispersion data, primarily from Yu & Mitchell (1979) and Schlue & Knopoff (1977), for average age ocean. Love- and Rayleigh-wave data extended to periods as short as 70 and 125 s, respectively, and to periods as long as 320 s. This covers the range of many previous isotropic inversions, inversions which have led to the conclusion that there is an extended region of very low shear velocity, 4.0–4.2 km s^{-1}, in the upper mantle. Although perturbations in the mantle below 220 km were allowed we anticipated that these would be small because the lower mantle structure already satisfied the gross Earth data set and we do not expect the average earth lower mantle to differ much from the oceanic lower mantle. In order to investigate the effect of anisotropy we have inverted this data set twice. In the first inversion we assumed that the mantle was isotropic. In the second

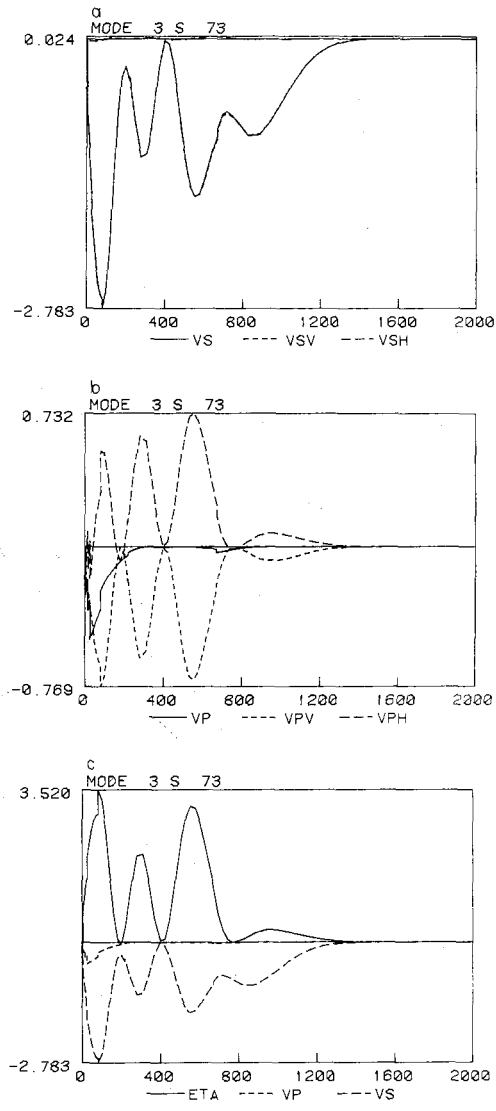

Figure 15. Same as Fig. 9 for mode ${}_3S_{73}$, period about 74 s.

inversion we allowed for the possibility of anisotropy. Since there are more free parameters in anisotropic models we allowed the isotropic model to have more flexibility by inverting for shear velocity and shear velocity gradient in the LID and LVZ. In the anisotropic model these two regions were perturbed together. Density was allowed to change throughout the Earth but the velocity structure was only perturbed above 670 km. The starting structure below 220 km was identical to model PREM which is based on a large normal mode and body wave data set. The perturbations in velocity were small, particularly for the anisotropic model, below 220 km.

Our previous experiments had shown that the shear velocities in the LID and LVZ were nearly continuous for anisotropic inversion. This is confirmed in the present study. The results are shown in Fig. 17. The upper panel shows the density perturbation which is much larger for the isotropic inversion than for the anisotropic inversion. The isotropic *P*-velocity

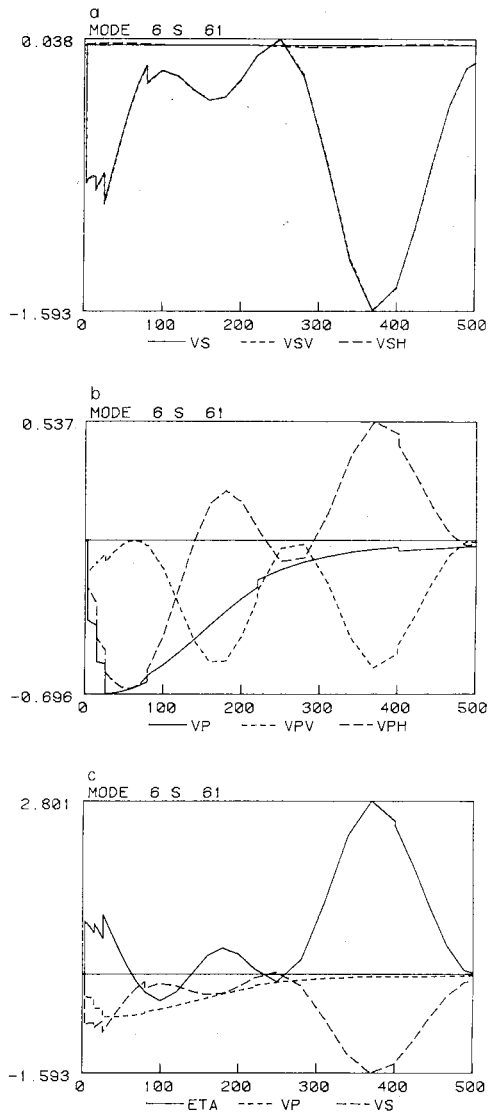

Figure 16. Same as Fig. 9 for mode ${}_6S_{61}$, period about 74 s.

in the upper mantle is close to the harmonic mean of the anisotropic *P*-wave velocities. Significant *P*-wave perturbations extend below 220 km for the isotopic model. Thus, the question of the depth extent of lateral variations is coupled to the problem of anisotropy of the upper mantle.

Whether anisotropy of the mantle is due to orientation of olivine, small-scale layering or oriented melt zones, anything that serves to increase the shear velocity along the symmetry axis will also increase the compressional velocity. Since the *PV* and *SV* partial derivatives have the same sign, the perturbations in shear velocity need not be as extreme as required in isotropic inversion. For example, if the trial model has Rayleigh-wave phase velocities which are higher than the data, the model may appear to require an extensive decrease in shear velocity and a marked LVZ. On the other hand, a moderate decrease in *SV* and *PV* and an increase in *PH* may accomplish the same purpose.

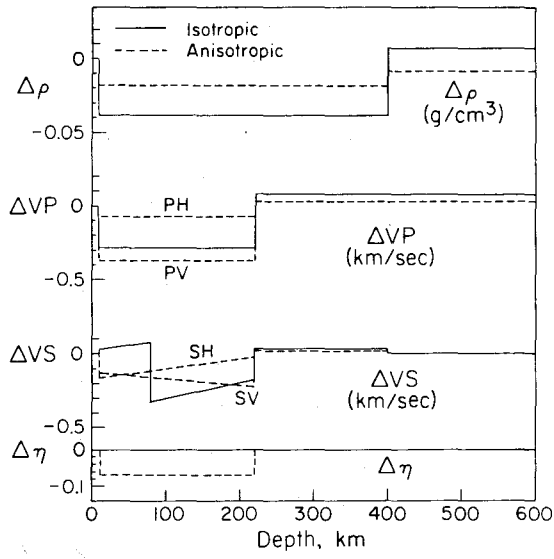

Figure 17. Results of numerical experiments illustrating the difference in perturbations of density and velocity resulting from the isotropic and anisotropic inversion of oceanic Love- and Rayleigh-wave data. The same data set and starting model are used in both inversions.

Similarly, the differences in dispersion between continents and oceans may appear to require deep differences in structure if isotropic partial derivatives form the basis for the inversion. If one or both of the structures are anisotropic they need only differ at relatively shallow depths (Anderson 1979).

Fig. 18 shows the upper mantle shear velocities in the anisotropic model PREM and velocities which are representative of isotropic inversion attempts. If only long-period data are inverted, > 70 s, the anisotropic inversions do not require a high-velocity LID. Short-period Rayleigh-wave data, not used in these examples, do require a thin high-velocity LID.

Discussion

We have shown that a small amount of anisotropy completely changes the nature of the surface wave and normal mode problem. In particular, the apparent lack of sensitivity of many of the spheroidal modes to the compressional velocity structure is due to the degeneracy in the isotropic case. The normal mode data set appears to be adequate to resolve the five elastic constants of a transversely isotropic upper mantle. Dziewonski & Anderson (1981) have shown that these data can be fitted with anisotropy restricted to the upper 200 km of the mantle. A few numerical experiments have demonstrated that anisotropic models fit the data better, removing the Rayleigh–Love discrepancy, and that the resulting models for the upper mantle are substantially different than the isotropic models. If Love- and Rayleigh-wave data cannot be satisfied by an isotropic model there is no recourse but to assume that at least five elastic constants control the dispersion. One cannot assume that toroidal and spheroidal modes are controlled by only one of the shear moduli or that Rayleigh waves are not sensitive to the compressional wave velocity.

The global data set, and regional Love- and Rayleigh-wave data are better fitted by a transversely anisotropic upper mantle than by conventional isotropic models. The increased number of elastic parameters is offset by the simpler structure, meaning that the improved

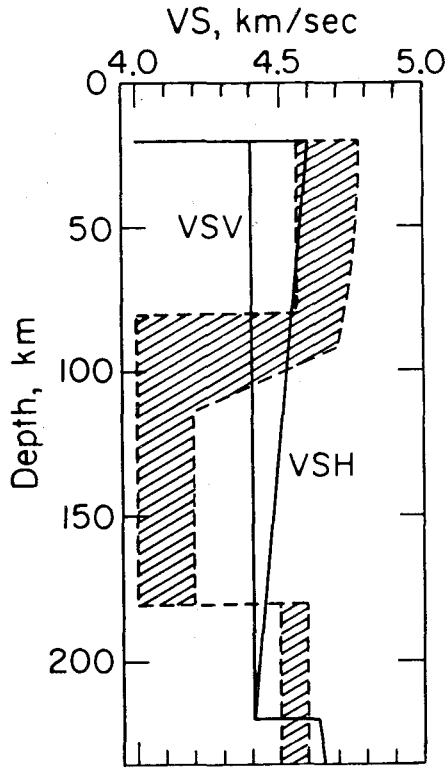

Figure 18. Vertical and horizontal shear velocities in PREM compared to upper mantle models resulting from isotropic inversion of surface wave and normal mode data. PREM also has *P*-wave anisotropy. Hatched area includes isotropic and pseudo-isotropic models of Schlue & Knopoff (1977), Forsyth (1975), Yu & Mitchell (1979) as well as those from the present study. *VSV* and *VSH* are controlled by independent elastic constants; the *P*- and *T*-derivatives can also be expected to be different, giving different gradients with depth. Crystal orientation can also change with depth.

fit is not a result of more degrees of freedom. It appears rather to be the result of a more appropriate parameterization. Because of the apparent pervasiveness of anisotropy it cannot be assumed that isotropic inversion of limited data sets, such as Rayleigh waves or *P*-waves, yield even approximately correct models for the upper mantle. Isotropy must be demonstrated by, for example, combined inversion of Love and Rayleigh waves, or *P*, *SH* and *SV* data. Lacking this, models which exhibit average shear velocities less than about 4.3 km s^{-1} in the upper mantle must be viewed with suspicion since we have found that data leading to such models can be explained by a small degree of anisotropy, anisotropy which is generally required by the broader data set.

In general, the spheroidal modes are more sensitive to *VSV* than to *VSH* but, as shown by Anderson (1961, 1966), this does not mean that an anisotropic structure can be approximated by an isotropic structure using the *VSV* velocity for the shear structure. The three compressional parameters η, *VPV* and *VPH* are also required. As a rule-of-thumb the compressional velocity is important at depths shallower than one-sixth of the wavelength in an isotropic structure. In an anisotropic structure the individual contributions of η, *VPV* and *VPH* persist to depths comparable to the depths influenced by the shear structure.

For the fundamental toroidal modes (Love waves) the controlling parameter is the horizontal *SH* velocity. The vertical shear wave velocity, *VSV*, however, is important for the

overtones. The partial derivatives as a function of depth oscillate and *VSV* and *VSH* are alternately important. The toroidal modes involve *SH* particle motion. The velocity, however, varies from *VSH* in the horizontal direction to *VSV* in the vertical, or radial direction. The toroidal overtones can be viewed as constructively interfering body waves; since the condition for constructive interference involves the wavelength and the angle of emergence it is clear that both components of velocity are important (Anderson 1962).

Acknowledgments

This research was supported by National Science Foundation Grants No. EAR77-14675, and EAR78-05353 and National Aeronautics and Space Administration Grant No. NSG-7610. We thank Brian Mitchell for preprints of his work with G. Yu. Contribution No. 3592, Division of Geological and Planetary Sciences, California Institute of Technology.

References

Aki, K., 1968. Seismological evidence for the existence of soft thin layers in the upper mantle under Japan, *J. geophys. Res.*, **73**, 585–594.

Akopyan, S., Zharkov, V. & Lyubimova, V., 1975. On the dynamic shear modulus of the Earth's interior, *Dokl. Akad. Nauk SSSR, 223.*

Anderson, D. L., 1961. Elastic wave propagation in layered anisotropic media, *J. geophys. Res.*, **66**, 2953–2963.

Anderson, D. L., 1962. Love wave dispersion in heterogeneous anisotropic media, *Geophysics*, **27**, 445–454.

Anderson, D. L., 1964. Universal dispersion tables. I. Love waves across oceans and continents on a spherical Earth, *Bull. seism. Soc. Am.*, **54**, 681–726.

Anderson, D. L., 1966. Recent evidence concerning the structure and composition of the Earth's mantle, *Phys. Chem. Earth*, **6**, 1–131.

Anderson, D. L., 1967. Latest information from seismic observations, in *The Earth's Mantle*, pp. 355–420, ed. Gaskell, T. F., Academic Press, New York.

Anderson D. L., 1979. Deep structure of continents, *J. geophys. Res.*, **84**, 7555–7560.

Anderson, D. L. & Harkrider, D., 1962. The effect of anisotropy on continental and oceanic surface wave dispersion (abstr.+), *J. geophys. Res.*, **67**, 1627.

Anderson, D. L. & Hart, R., 1976a. An Earth model based on free oscillations and body wave, *J. geophys. Res.*, **81**, 1461.

Anderson, D. L. & Hart, R., 1976b. Absorption and the low velocity zone, *Nature*, **263**, 397–398.

Anderson, D. L., Kanamori, H., Hart, R. S. & Liu, H.-P., 1976. The earth as a seismic absorption band, *Science*, **196**, 1104–1106.

Anderson, D. L., Minster, B. & Cole, D., 1974. The effect of oriented cracks on seismic velocities, *J. geophys. Res.*, **79**, 4011–4015.

Anderson, D. L. & Toksöz, M. N., 1963. Surface wave on a spherical Earth, *J. geophys. Res.*, **68**, 3483–3500.

Ando, M., Ishikawa, Y. & Wada, H., 1980. *S*-wave anisotropy in the upper mantle under a volcanic area in Japan, *Nature*, **286**, 43–46.

Backus, G. E., 1962. Long-wave seismic anisotropy produced by horizontal layering, *J. geophys. Res.*, **67**, 4427–4440.

Bamford, D., 1977. P_n velocity anisotropy in a continental upper mantle, *Geophys. J.*, **49**, 29–48.

Bibee, L. D. & Shor, G. G., 1976. Compressional wave anisotropy in the crust and upper mantle, *Geophys. Res. Lett.*, **3**, 639–642.

Brune, J. & Dorman, J., 1963. Seismic waves and earth structure in the Canadian shield, *Bull. seism. Soc. Am.*, **53**, 167–209.

Christensen, N. I. & Crosson, R. S., 1968. Seismic anisotropy in the upper mantle, *Tectonophys.*, **6**, 93–107.

Christensen, N. I. & Salisbury, M., 1979. Seismic anisotropy in the oceanic upper mantle: evidence from the Bay of Islands ophiolite, *J. geophys. Res.*, **84**, 4601–4610.

Dziewonski, A. & Anderson, D. L., 1981. Preliminary reference Earth model, *Phys. Earth planet. Int.*, **25**, 297–356.

Dziewonski, A., Hales, A. & Lapwood, E., 1975. Parametically simple Earth models consistent with geophysical data, *Phys. Earth planet. Int.*, **10**, 12–48.

Forsyth, D. S., 1975. The early structural evolution and anisotropy of the oceanic upper mantle, *Geophys. J.*, **43**, 103–162.

Gilbert, F. & Dziewonski, A., 1975. An application of normal mode theory to the retrieval of structural parameters and source mechanisms from seismic spectra, *Phil. Trans. R. Soc. A*, **278**, 187–269.

Harkrider, D. B. & Anderson, D. L., 1962. Computation of surface wave dispersion for multilayered anisotropic media, *Bull. seism. Soc. Am.*, **52**, 321–332.

Hart, R., Anderson, D. L. & Kanamori, H., 1977. The effect of attenuation on gross Earth models, *J. geophys. Res.*, **82**, 1647–1654.

Hess, H., 1964. Seismic anisotropy of the uppermost mantle under oceans, *Nature*, **203**, 629.

Hirn, A., 1977. Anisotropy in the continental upper mantle: possible evidence from explosion seismology, *Geophys. J.*, **49**, 49–58.

Jeffreys, H., 1961. Small corrections in the theory of the surface waves, *Geophys. J.*, **6**, 115–117.

Jeffreys, H., 1965. Damping of *S* waves, *Nature*, **208**, 675.

Jordan, T. & Anderson, D. L., 1974. Earth structure from free oscillations and travel-times, *Geophys. J.*, **36**, 411.

Kanamori, H. & Anderson, D. L., 1977. Importance of physical dispersion in surface wave and free oscillation problems; review, *Rev. Geophys. Space Phys.*, **15**, 105–112.

Liu, H.-P., Anderson, D. L. & Kanamori, H., 1976. Velocity dispersion due to anelasticity implications for seismology and mantle composition, *Geophys. J.*, **47**, 41–58.

McEvilly, T. V., 1964. Central U.S. crust–upper mantle structure from Love and Rayleigh wave phase velocity inversion, *Bull. seism. Soc. Am.*, **54**, 1997–2016.

Peselnick, L. & Nicolas, A., 1978. Seismic anisotropy in an ophiolite periodotite: application to oceanic upper mantle, *J. geophys. Res.*, **83**, 1227–1235.

Postma, G. W., 1955. Wave propagation in a stratified medium, *Geophysics*, **20**, 780–806.

Raitt, R. W., Shor, G. G. & Morris, G. B., 1971. Mantle anisotropy in the Pacific Ocean, *Tectonophys.*, **12**, 173.

Randall, M. J., 1976. Attenuative dispersion and frequency shifts of the Earth's free oscillations, *Phys. Earth planet. Int.*, **12**, 1.

Schlue, J. W. & Knopoff, L., 1977. Shear wave polarization anisotropy in the Pacific Basin, *Geophys. J.*, **49**, 45–165.

Takeuchi, H. & Saito, M., 1972. Seismic surface waves, in *Methods in Computational Physics*, **11**, 217–295, Academic Press, New York.

Thatcher, W. & Brune, J. N., 1969. Higher-mode interference and observed anomalous apparent Love wave phase velocities, *J. geophys. Res.*, **74**, 6603–6611.

Toksöz, M. N. & Anderson, D. L., 1963. Generalized two-dimensional model seismology with application to anisotropic Earth models, *J. geophys. Res.*, **68**, 1121–1130.

Yu, G. K. & Mitchell, B. J., 1979. Regionalized shear velocity models of the Pacific upper mantle from observed Love and Rayleigh wave dispersion, *Geophys. J.*, **57**, 311–341.

Appendix: partial derivatives for a transversely isotropic earth

Following Dziewonski & Anderson (1981), who used elements of theory developed by Takeuchi & Saito (1972), a relative change in the squared eigenfrequency of a normal mode is:

$$\frac{\delta\omega^2}{\delta\omega} = \int_0^1 r^2 dr(\tilde{A}\cdot\delta A + \tilde{C}\cdot\delta C + \tilde{F}\cdot\delta F + \tilde{L}\cdot\delta L + \tilde{N}\cdot\delta N + \tilde{R}\cdot d\rho) \tag{A1}$$

for the transversely isotropic case, and:

$$\frac{\delta\omega^2}{\omega^2} = \int_0^1 r^2 dr(\tilde{K}\cdot\delta K + \tilde{M}\cdot\delta\mu + \tilde{R}\cdot\delta\rho) \tag{A2}$$

for the isotropic case.

The differential kernels with respect to perturbations in the elastic parameters in equations (A1) and (A2) can be expressed in terms of eigenfunctions $U(r)$, $V(r)$ and their derivatives with respect to the radius (designated by a dot) and the angular order number l:

$$\tilde{C} = \dot{U}^2; \tag{A3a}$$

$$\tilde{A} = r^{-2}[2U - l(l+1)V]^2; \tag{A3b}$$

$$\tilde{F} = 2r^{-1}\dot{U}[2U - l(l+1)V]; \tag{A3c}$$

$$\tilde{L} = l(l+1)[\dot{V} + (U - V)/r]^2; \tag{A3d}$$

$$\tilde{N} = r^{-2}\{(l+2)(l+1)l(l-1)V^2 - [2U - l(l+1)V]^2\}; \tag{A3e}$$

$$\tilde{K} = \{\dot{U} + r^{-1}[2U - l(l+1)V]\}^2 = \tilde{A} + \tilde{C} + \tilde{F}; \tag{A3f}$$

$$\tilde{M} = \tilde{L} + \tilde{N} + 2/3(2\tilde{A} + 2\tilde{C} - \tilde{F}). \tag{A3g}$$

The eigenfunctions are normalized:

$$\omega^2 \int_0^1 \rho[v^2 + l(l+1)V^2] r^2 dr = 1. \tag{A4}$$

The partial derivatives for toroidal modes are:

$$\tilde{L} = l(l+1)(\dot{W} - W/r)^2; \tag{A5a}$$

$$\tilde{N} = (l+2)(l+1)l(l-1)(W/r)^2; \tag{A5b}$$

$$\tilde{M} = \tilde{L} + \tilde{N}; \tag{A5c}$$

where $W(r)$ is the normalized scalar displacement function:

$$l(l+1)\omega^2 \int_0^1 \rho W^2 r^2 dr = 1. \tag{A6}$$

The figures with partial derivatives shown in this paper correspond to perturbations in the relative period of a normal mode with respect to the velocities or parameter η:

$$\frac{\delta T}{T} = \int_0^1 dr(R' \cdot \delta\rho + \tilde{P}_V \cdot \delta V_{PV} + \tilde{P}_H \cdot \delta V_{PH} + \tilde{S}_V \cdot \delta V_{SV} + \tilde{S}_H \cdot \delta V_{SH} + \tilde{E} \cdot \delta\eta) \tag{A7}$$

or

$$\frac{\delta T}{T} = \int_0^1 dr(R'' \cdot \delta\rho + \tilde{P} \cdot \delta V_P + \tilde{S}\delta V_S) \tag{A8}$$

for the anisotropic and isotropic cases, respectively, where:

$$\tilde{P}_V = -r^2 \rho V_{PV} \tilde{C}; \tag{A9a}$$

$$\tilde{P}_H = -r^2 \rho V_{PH}(\tilde{A} + \eta\tilde{F}); \tag{A9b}$$

$$\tilde{S}_V = -r^2 \rho V_{SV}(\tilde{L} - 2\eta\tilde{F}); \tag{A9c}$$

$$\tilde{S}_H = -r^2 \rho V_{SH}\tilde{N}; \tag{A9d}$$

$$\tilde{E} = -(1/2)r^2 \rho \tilde{F}(V_{PH}^2 - 2V_{SV}^2); \tag{A9e}$$

$$\tilde{P} = -r^2 \rho V_P \tilde{K}; \tag{A9f}$$

$$\tilde{S} = -r^2 \rho V_S(\tilde{M} - 4\tilde{K}/3); \tag{A9g}$$

the density kernels, R' and R'', are given by Dziewonski & Anderson (1981) in equations (A6) and (A9).

One should notice that for the isotropic case:

$$\tilde{P} = \tilde{P}_V + \tilde{P}_H = -r^2 \rho V_P(\tilde{A} + \tilde{C} + \tilde{F});$$

as $\eta = 1$ and $V_{PV} = V_{PH}$. Thus $\tilde{P}$ can be small, even though the absolute values of $\tilde{A}$, $\tilde{C}$ and $\tilde{F}$ may be large. For this to occur we must have, from (A3f):

$$\dot{U} \sim -r^{-1}[2U - l(l+1)V]. \tag{10}$$

In this case $\tilde{A} \sim \tilde{C}$ and $\tilde{A} \sim -\tilde{F}/2$. Assuming $V_{PV} \sim V_{PH}$ and $\eta \sim 1$, we have $\tilde{P}_H \sim -\tilde{P}_V$ and $\tilde{E}$ should be proportional to $\tilde{P}_H$ and of the same sign.

This is indeed what happens: the density of compressional energy, $K \cdot \tilde{K}$ (proportional to the trace of the strain tensor) is small below the turning point for the *P*-waves, although the individual diagonal elements of this tensor are, in general, quite large. Thus, introduction of transverse isotropy increases the range of depths for which perturbations in compressional velocities are of importance.

In order to understand the different sensitivities of the toroidal and spheroidal modes to perturbations in V_{SH}, one should notice that the expression (A3e) for $\tilde{N}$ consists of the difference of two terms. Assuming that $|U| \ll l(l+1)|V|$, a condition generally satisfied for mantle modes and large values of l, the partial $\tilde{N}$ is approximately $-2l(l+1)(V/r)^2$, while the original expression contained terms in l^4. For toroidal modes, equation (A5b), there is no such cancellation, and therefore, the senstivitiy of toroidal modes with respect to perturbations in V_{SH} is high. Both types of modes are sensitive to perturbations in $\tilde{S}_V$, except at the free surface, where $\tilde{L}$ is zero; the fundamental toroidal mode is an exception: $(\dot{W} - W/r)^2$ is, for $l > 10$, relatively small in comparison with $l^2(W/r)^2$ at all depths.

The relatively small values of $\tilde{N}$ for spheroidal modes explain another feature of partial derivatives for shear velocities. For overtones, both the tangential strain and the horizontal displacement may have zero crossings, i.e. $\tilde{L}$ and $\tilde{N}$ are zero, respectively. The positions of these zero crossings are shifted, so that where strain is zero, the displacement is maximum and *vice versa*. For toroidal modes, the sum of $\tilde{L}$ and $\tilde{N}$ yields a relatively smooth function, with a maximum near the turning point. Thus, partials for toroidal overtones are similar in character to the partials of travel times with respect to perturbations in velocity. On the other hand, for spheroidal overtones the kernel $\tilde{N}$ is negligible, and the zeros in $\tilde{L}$ are important. Thus, even though for the isotropic case the *SV*- and *SH*-waves to which these modes correspond in the asymptotic limit, and for low enough phase velocities, should have identical properties, the partial derivatives for *individual modes* have a significantly different character.